Supporting Information

Single-Nanowire Electrochemical Probe Detection for Internally Optimized Mechanism of Porous Graphene in Electrochemical Devices

Ping Hu, [‡] ***Mengyu Yan,*** [‡] ***Xuanpeng Wang, Chunhua Han,* Liang He, Xiujuan Wei, Chaojiang Niu, Kangning Zhao, Xiaocong Tian, Qiulong Wei, Zijia Li and Liqiang Mai*.***

State Key Laboratory of Advanced Technology for Materials Synthesis and Processing, Wuhan University of Technology, Wuhan 430070, China

Corresponding Authors

* E-mail: (L.M.) mlq518@whut.edu.cn.

* E-mail: (C.H.) hch5927@whut.edu.cn.

Experimental

1. Synthesis of MnO_2, MnO_2/rGO, and MnO_2/pGO nanowires

The MnO_2/rGO nanowires were produced by the hydrothermal method. In a typical synthesis, 2 mmol $KMnO_4$, 2 mmol NH_4F and 2 ml of rGO suspension (~2 mg/ml) were added to 80 ml of distilled water and magnetically stirred at room temperature for 20 min. The sample was then placed into a 100 ml autoclave and heated at 180℃ for 24 h. After the sample was washed and dried, a brownish-black powder was obtained. The pure MnO_2 nanowires were prepared using the same method described above without the addition of rGO. Then, we dealt MnO_2/rGO with 10 mmol/L hydrazine hydrate for different times, including 1, 2, 3, 6, 12, and 24 hours. For improved structure and capacity over the different hydrazine hydrate MnO_2/rGO nanowires, we chose to hydrate for 3 hours to produce the MnO_2/pGO nanowires.

2. Structure Characterization

X-ray diffraction (XRD) measurements were performed to investigate crystallographic information using a D8 Discover X-ray diffractometer with a non-monochromated Cu Kα X-ray source. Field-emission scanning electron microscopic (FESEM) images were collected using a JSM-7001F microscope at an acceleration voltage of 10 kV. Transmission electron microscopic (TEM) and high-resolution TEM images were recorded with a JSM-2100F STEM/EDS microscope. The X-ray photoelectron (XPS) spectra were recorded on a Shimadzu Axis Ultra

spectrometer with an Mg Kα = 1253.6 eV excitation source. An Autolab 302N Probe Station (Lake Shore, TTPX) and Semiconductor Characterization System (Agilent, B1500A) were used to test the electrochemical performances of the single-nanowire devices.

3. Fabrication of Single-Nanowire Electrochemical Devices

Our manganese dioxide single-nanowire electrochemical device is configured with one single nanowire as a cathode, one flake of Au as an anode, and KOH (6 mol/L) as an electrolyte. The single-nanowire devices were fabricated by the following steps. EBL patterning of contact pads was performed on a highly doped silicon wafer with 300 nm SiO_2, followed by developing, rinsing, Cr/Au (5/50 nm) deposition by thermal evaporation, and then lift-off. The prepared MnO_2 NWs were then deposited on the substrate by contacting the MnO_2 nanowires and contact pad with Cr/Au electrode through EBL patterning, developing, rinsing, Cr/Au (5/150 nm) deposition by thermal evaporation, and then lift-off. A probe station was used for air characterization to check the I-V cyclic voltammetry performances of the MnO_2 NWs. EBL patterning and developing of SU-8 2002 was used to create the isolation layer of the gold electrode to avoid leakage current. A drop of KOH (6 mol/L) electrolyte was used to coat the nanowire and the counter electrode (Au). The performance of the device was then tested. Furthermore, two other single-nanowire devices were fabricated by the same processes.

4. Electrochemical Characterization

For electrochemical characterization, the electrochemical performances of these single-nanowire electrochemical devices were measured by Autolab. The different single-nanowire electrochemical devices were fabricated using a mechanical shaping process modified from a previous method adopted to fabricate graphene-based, single-nanowire electrochemical devices. Electrochemical performances of the single-nanowire electrochemical devices were investigated in a two-electrode system using a cyclic voltammetry station and I-V properties. The scan rate of the CV response varied from 20 to 500 mV/s with a potential range from 0 to 0.8 V.

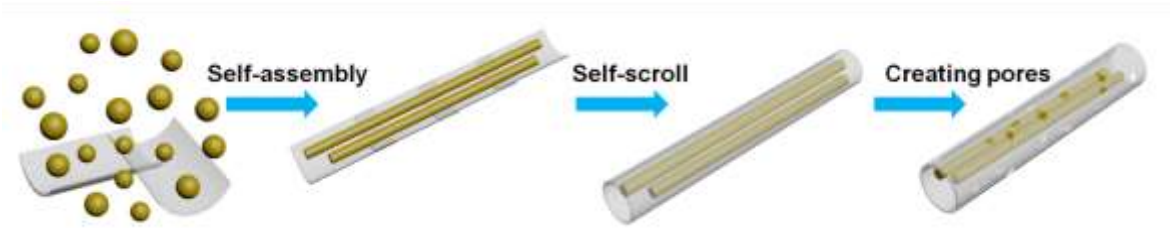

Figure S1. The construction processes of MnO_2/pGO wire-in-scroll NWs. The brown dots represent the precursor of nanowire template, which forms the nanowires after hydrothermal processes. The gray sheets and scroll represent reduced graphene oxide.

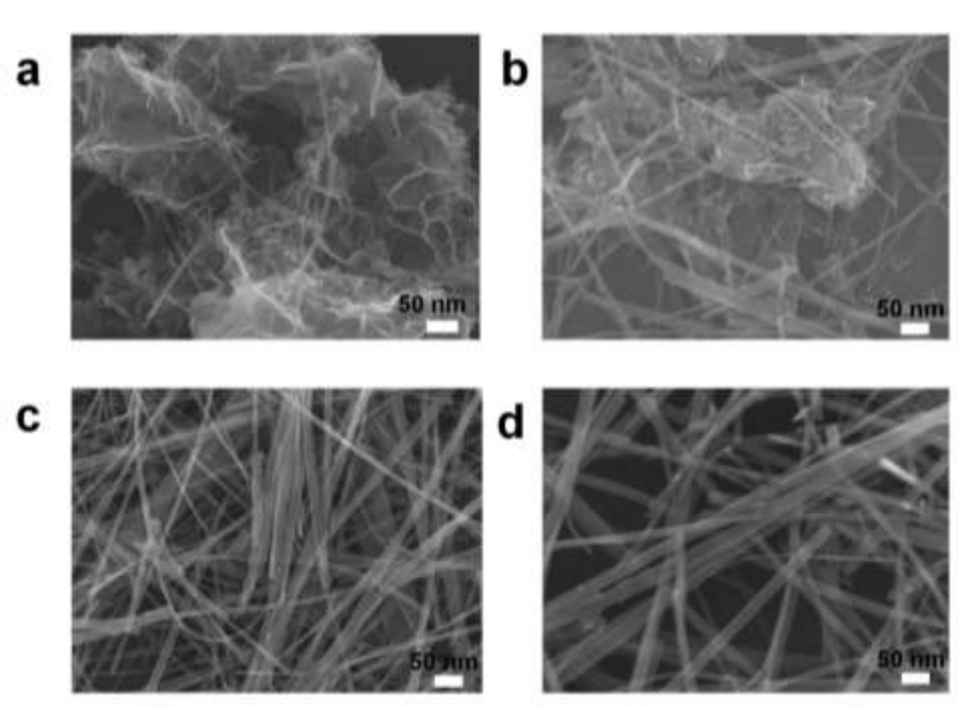

Figure S2. SEM images of different MnO_2/rGO NWs produced by different hydrothermal times: (a) 3 h, (b) 6 h, (c) 12 h, (d) 18 h.

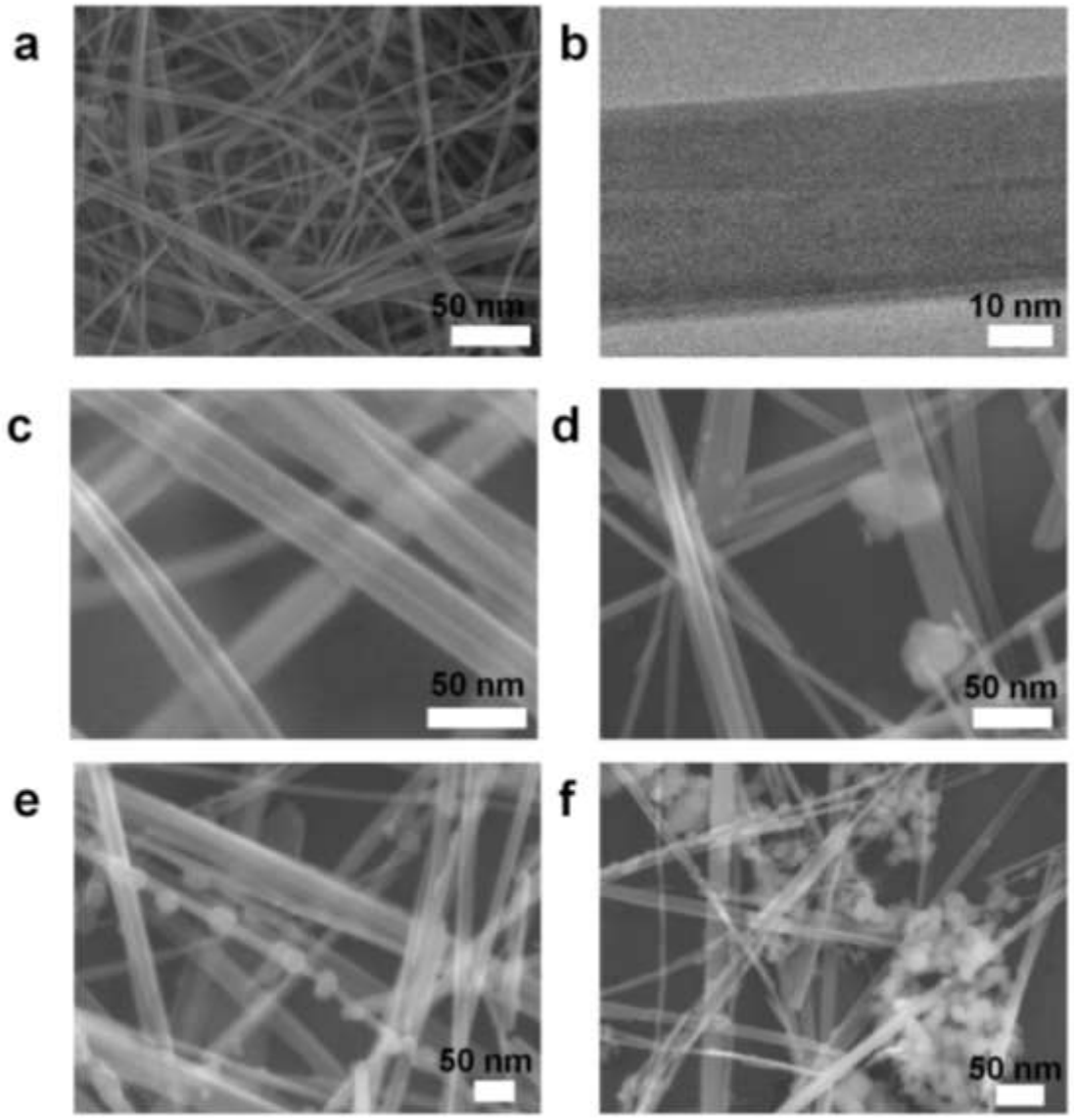

Figure S3. (a,b) SEM and TEM images of MnO_2. (c) SEM image of MnO_2/rGO. (d-f) SEM images of MnO_2/rGO dealt with 10 mmol/L of hydrazine hydrate for different times: (d) 6h (MnO_2-rGO-6h), (e) 12h (MnO_2-rGO-12h), (f) 24 h (MnO_2-rGO-24h).

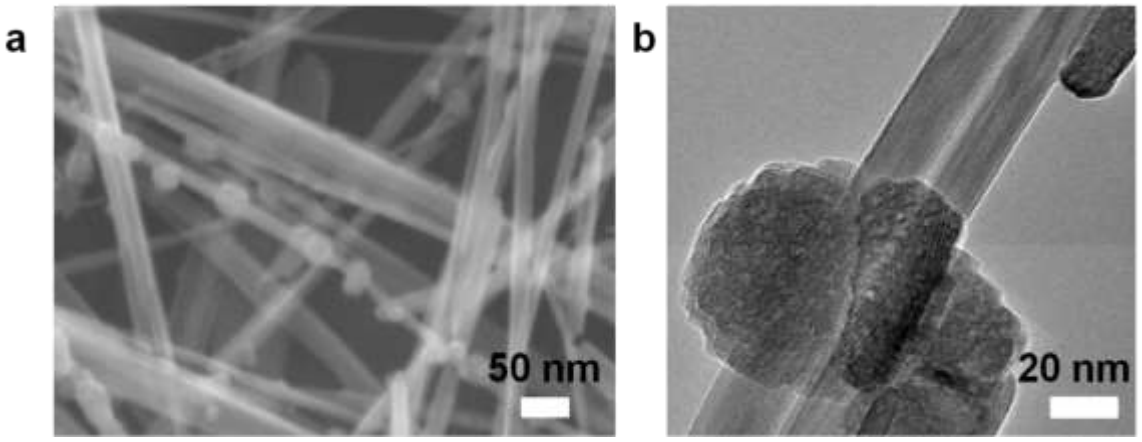

Figure S4. (a) SEM image of MnO_2-rGO-12h. (b) TEM image of MnO_2-rGO-12h.

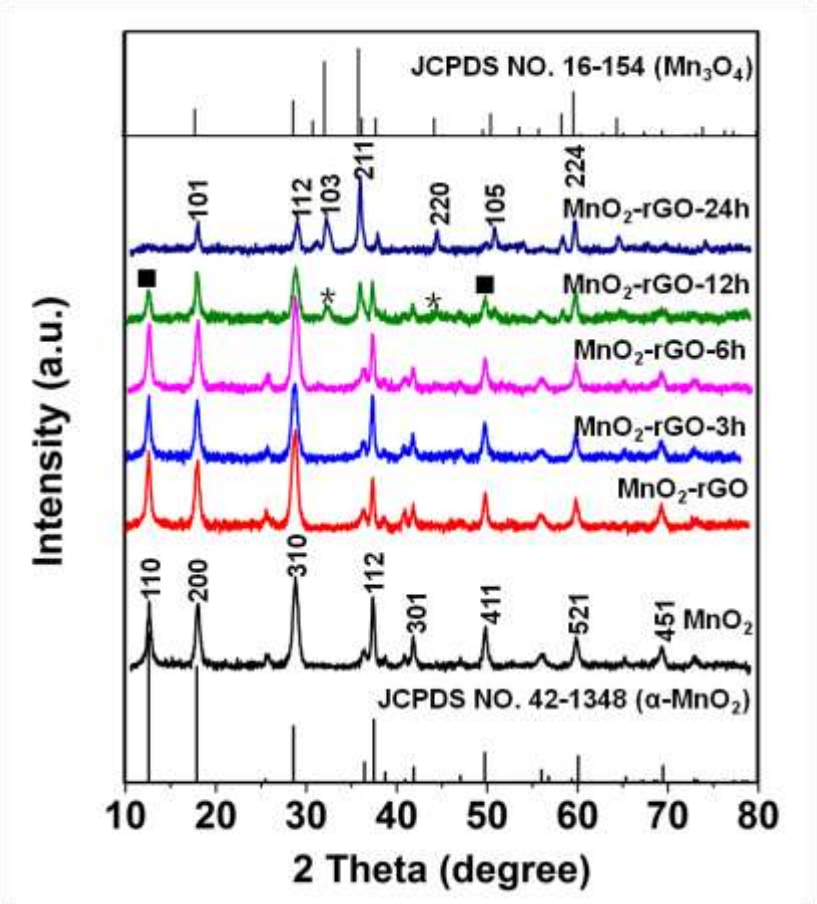

Figure S5. The XRD patterns of MnO_2, MnO_2/rGO, MnO_2-rGO-3h (MnO_2/pGO), MnO_2-rGO-6h, MnO_2-rGO-12h and MnO_2-rGO-24h.

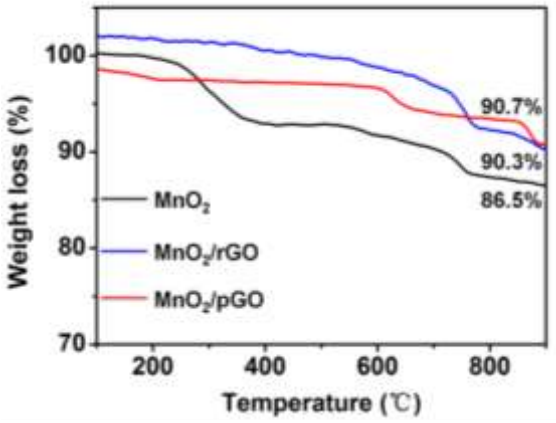

Figure S6. The TG curves of MnO_2, MnO_2/rGO and MnO_2/pGO NWs.

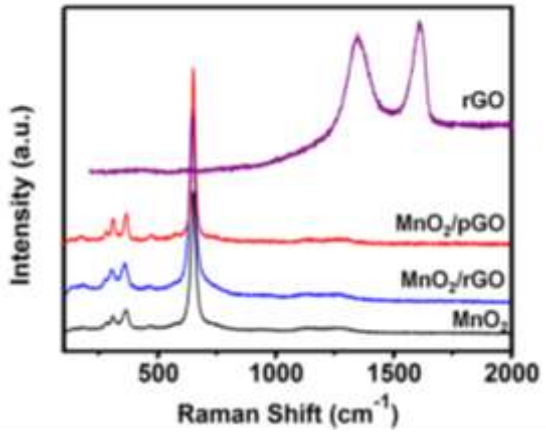

Figure S7. The Raman spectra of MnO_2, MnO_2/rGO, MnO_2/pGO NWs and rGO, showing no obvious shifts among the MnO_2, MnO_2/rGO and MnO_2/pGO NWs. Due to the small content of graphene (3.38 wt%), the D and G shifts between MnO_2/rGO and MnO_2/pGO NWs are not obvious.

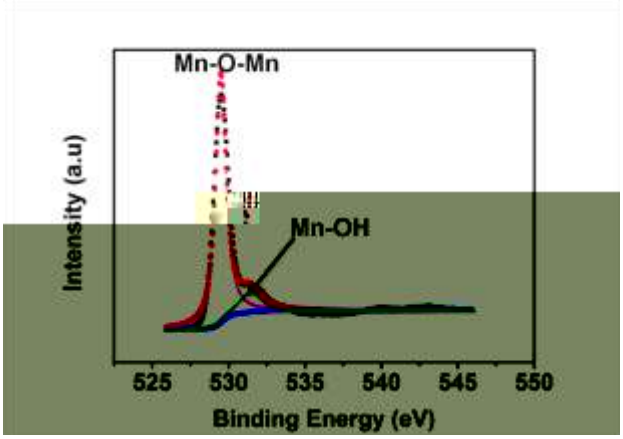

Figure S8. The O 1s XPS spectrum of MnO_2. The O 1s core level spectrum is used to confirm the presence of oxygen vacancies in MnO_2. The spectra can be fit with two components, which are related to the Mn-O-Mn bond (529.7 eV) of tetravalent oxide and the Mn-OH bond (531.43 eV) of hydrated trivalent oxide. Quantitative analysis shows that oxygen vacancies exist in MnO_2 because of the proportion of Mn^{3+} in MnO_2 (13.84%).

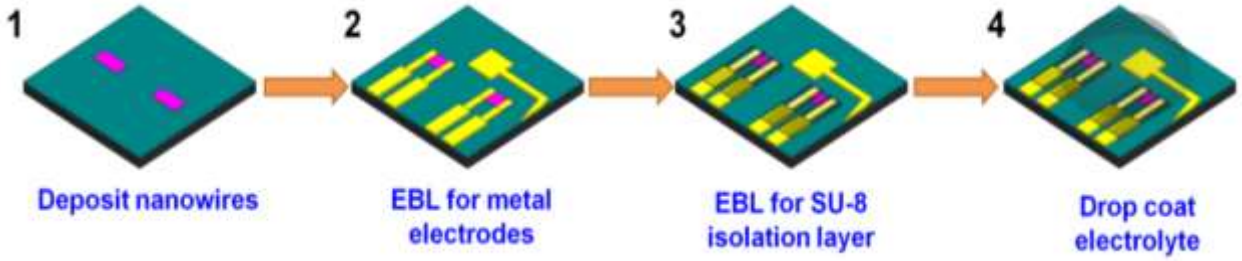

Figure S9. The fabrication processes of dropping electrolyte coating on a single-nanowire electrochemical device. The processes involve four steps. Step 1. EBL patterning of contact pads on a highly doped silicon wafer with 300 nm of SiO_2, followed by developing, rinsing, Cr/Au (5/50 nm) deposition by thermal evaporation, and lift-off. The prepared MnO_2, MnO_2/rGO and MnO_2/pGO NWs are deposited on the substrate. Step 2. Contacting the nanowires and contact pad with Cr/Au electrode through EBL patterning, developing, rinsing, Cr/Au (5/150 nm) deposition by thermal evaporation, and lift-off. Step 3. Using a probe station for air characterization to check the I-V cyclic voltammetry performance of the MnO_2, MnO_2/rGO and MnO_2/pGO NWs. EBL patterning and developing of SU-8 2002 as an isolation layer of the gold

electrode to avoid leakage current. Step 4. Drop coating the KOH (6 mol/L) electrolyte on the nanowire and the counter electrode (Au), and test the performance of device.

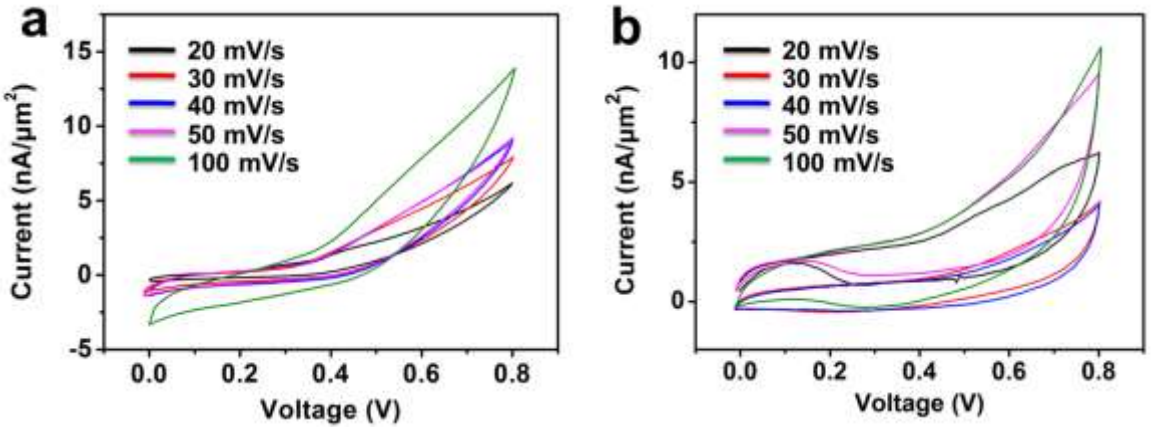

Figure S10. The CV curves at scan rates of 20, 30, 40, 50, and 100 mV/s for the as-prepared MnO_2 and MnO_2/rGO single-nanowire electrochemical devices in 6 mol/L KOH.

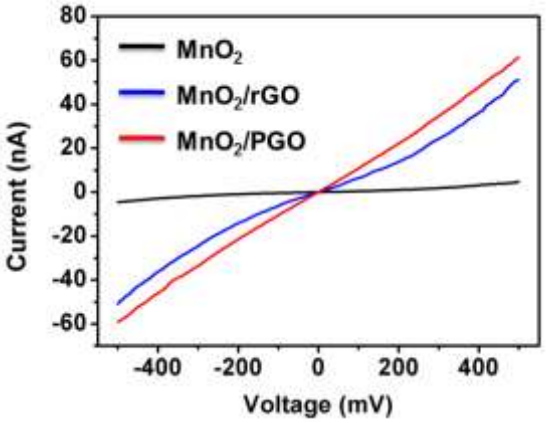

Figure S11. The single-nanowire transport properties of the MnO_2, MnO_2/rGO and MnO_2/pGO NWs.

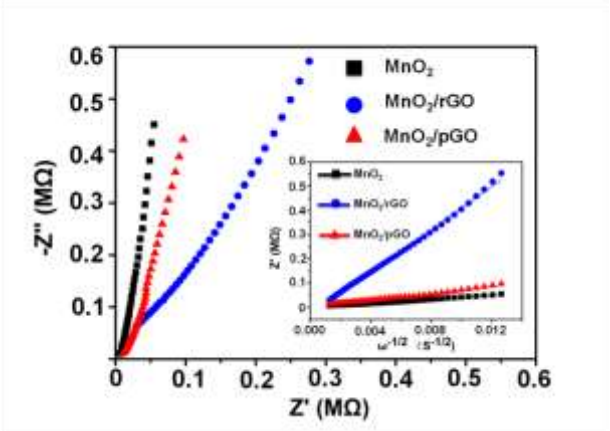

Figure S12. Nyquist plots of MnO_2, MnO_2/rGO and MnO_2/pGO in a frequency regime from 1 to 100 kHz with a three-electrode system. The EIS measurements are performed in an aqueous solution of 6 mol/L KOH.

The ion diffusion coefficient can also be calculated using the following equation:

$$D = R^2T^2 / 2A^2n^4F^4C^2\sigma^2$$

where R represents the gas constant, T represents the absolute temperature, A represents the surface area of the anode (cm^2), n represents the number of electrons transferred in the half-reaction for the redox couple (2), F represents the Faraday constant, C represents the concentration of ions in the solid, D represents the diffusion coefficient (cm^2/s), and σ represents the Warburg factor relative to Z_{re}. From the slope of the lines in the inset, σ can be obtained.

$$Z_{re} = R_D + R_L + \sigma\omega^{-1/2}$$

According to the linear fit, the slope of the real part of the complex impedance is versus $\omega^{-1/2}$ (The response of AC impedance changes noisily when the frequency is below 10^3 Hz. Only impedance data in the frequency range of 10^3~10^6 Hz is stable in the single-nanowire system.) at the potential of 0.3 V (*vs* HgCl/Hg) for MnO_2, MnO_2/rGO and MnO_2/pGO NWs are 4.08×10^6, 4.39×10^7 and 7.06×10^6, respectively. The ions diffusion coefficients at room temperature are calculated to be 5.55×10^{-8}, 5.21×10^{-9} and 2.31×10^{-8} cm^2/s for the MnO_2, MnO_2/rGO and MnO_2/pGO NW, respectively.

In general, the EIS contains R_{con}, R_{ct}, and R_w. In this single-nanowire device system, the nanowire is surrounded by electrolyte, so ions are very easily transported to the interface of the active material. According to our understanding, the frequency of 10^6 Hz corresponds to R_{ct},

which may be due to the fast ion diffusion in our system. R_{con} and R_{ct} cannot be tested with Autolab 302N because of the upper frequency limitation. Only R_w can be calculated. In this way, the ion diffusion coefficients, which are calculated from the EIS, support our assertions in the manuscript.

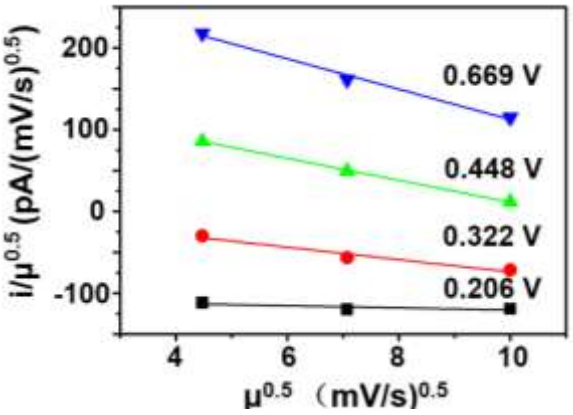

Figure S13. The plots of $\mu^{0.5}$ *vs* $i/\mu^{0.5}$ used for calculating constants k_1 and k_2 at different potentials from a variety of cathodic voltammetric sweeps. According to a power law relationship, $I = k\mu$ for non-diffusion limited processes and $i = k\mu^{0.5}$ for diffusion limited processes. Thus, total current $i(V) = k_1\mu + k_2\mu^{0.5}$ and $i(V) / \mu^{0.5} = k_1\mu^{0.5} + k_2$ at different potentials are calculated from cyclic voltammograms at different scan rates ranging from 20 to 500 mV/s. Plots of $i/\mu^{0.5}$ *vs* $\mu^{0.5}$ have been drawn at a variety of potentials. The k_1 (slope) and k_2 (intercept) are calculated from the straight line.

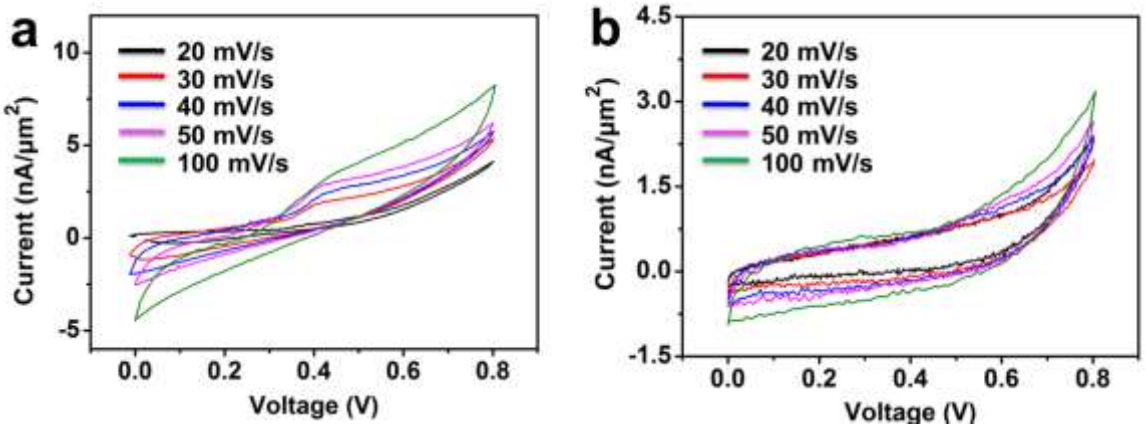

Figure S14. The CV curves at scan rates of 20, 30, 40, 50, and 100 mV/s for the as-prepared MnO_2 and MnO_2/rGO symmetric single-nanowire electrochemical devices in 6 mol/L KOH.

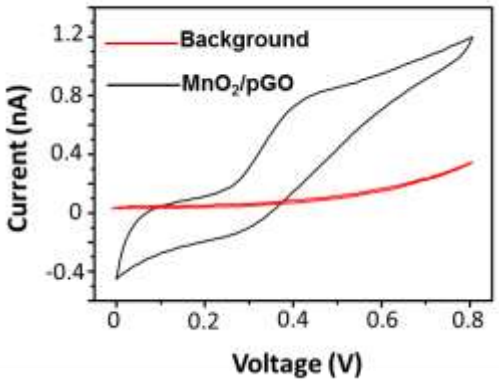

Figure S15. The CV curves at a scan rate of 100 mV/s for the MnO_2/pGO symmetric single-nanowire electrochemical devices and background device in 6 mol/L KOH.